TFEC9-1268

ADDED MASS MOMENT OF INERTIA OF A ROTATIONALLY OSCILLATING SURFACE-PIERCING CIRCULAR CYLINDER IN STILL WATER

Hamid Arionfard[1], Yoshiki Nishi[1*]

[1]Department of Systems Design for Ocean-Space, Yokohama National University, Japan

ABSTRACT

A mechanical apparatus is built to investigate the added mass moment of inertia (AMI) of a circular cylinder with diameter D, which is pivoted vertically at distance l from its central axis. A numerical model is developed to estimate the AMI based on the experimental results recorded from a free decay tests in water. Then a simulation technique based on optimization is used to estimate the parameters such that the difference between simulated model output and experimental data is minimized. This method improves estimates of the AMI by considering the nonlinear effects of damping and large angular displacements.
The tests are conducted with different initial displacements (Θ0), different distances from the bottom wall boundary (hg) and different arm length ratios (L*=l/D). Moreover, three hypotheses are made to estimate the AMI numerically and then compared to the experimental results.
Although the outputs of all hypotheses converge to the experimental data for L*>1, assuming a cylindrical tube of water moving with the cylinder, produces the most accurate results.
The free decay tests where the end of the cylinder is close to the wall boundary produces almost identical results regardless of the gap ratio. Hence, the bed proximity effect is not significant in this study.
Free decay tests are conducted with Θ0=10°,30° and 60° to study the effect of the initial displacement. It has been found that the calculated AMI based on potential flow theory is reliable for an initial displacement less than 10° but the effect of shear drag force should be considered for an initial displacement more than 10°.

KEYWORDS: Added mass, Added mass moment of inertia, Oscillating cylinder, Pivoted cylinder.

1. INTRODUCTION

Whenever acceleration is imposed on fluid by acceleration of a body moving through it, or acceleration of the fluid relative to the body, additional inertial force acts on the body due to the 'added mass' effect. The calculation of these inertial forces has been of fundamental interest in fluid mechanics for more than a century. It was first given an exact mathematical interpretation by Green and Stokes in 1833 and 1843 (Lamb, 1959). They evaluated the added mass of a sphere in rectilinear accelerating motion in an ideal fluid of infinite extent. Perhaps the simplest view of the phenomenon of added mass is that it determines the necessary work done to change the kinetic energy associated with the motion of the fluid. Any motion of fluid such as that which occurs when a body moves through it implies a certain positive, non-zero amount of kinetic energy associated with the fluid motions.

In mathematical hydrodynamics, it is perfectly correct to say that the entire effect produced by the presence of the fluid may be represented by a mass which is to be added to the mass of the moving body as an added mass accelerated with the body. It ought to be noted that such an identifiable fluid mass does not exist. In fact, the entire fluid is accelerating to some degree to increase the total kinetic energy of the fluid (in reality due to the inherent viscosity of real fluids the fluid acceleration attenuates quickly within a finite volume).

*Corresponding Author: phone: +81 45 339 4087; fax: +81 45 339 4099; e-mail: nishi-yoshiki-rg@ynu.ac.jp

Unlike a transitional motion where the exact distribution of the added mass is insignificant, in a rotational motion the distribution of the fluid moving with the object affects the mass moment of inertia (AMI). When a body vibrates rotationally in a fluid, an effect equivalent to an increase in the mass moment of inertia comes into play. Several theories have been proposed to explain the added mass and AMI but the simplest method is using potential flow hypothesis based on the pressure distribution over the object (Wendel, 1950).

Thus far, hydrodynamic moments of inertia have been calculated for many typical cross sections of elliptical, square (Proudman, 1916) or regular octagon (Weinblum, 1931). However, the AMI turns out to zero when a circular cylinder rotationally vibrates around its central axis or when a sphere vibrates around its center point based on potential flow hypothesis (Melorose et al., 2015).

Recently, considerable attention has been paid to the rotational motion of a cylinder around a pivot point. Some examples of application are riser pipes analysis, vortex induced vibration of a pivoted cylinder (Flemming and Williamson, 2005) and energy harvesting from instability of pivoted cylinders (Sung et al., 2015). Understanding the behavior of rotational vibration of a circular cylinder needs a better estimation for AMI. To the author´s best knowledge, very few publications are available in the literature that address the estimation of the AMI of a circular cylinder specifically around the central axis.

In the present study, we investigate the AMI of a vertically pivoted surface-piercing circular cylinder undergoing rotational oscillation. In most of relevant experimental researches, added mass has been evaluated at the resonant frequency corresponding to the peak of a frequency-response curve obtained from a “forced” vibration analysis. In this paper, we follow a simpler approach where a “free” vibration responses instead of a “forced” ones were used to determine the added mass moment of inertia (Wu and Hsieh, 2001).

The present paper is organized as follows. The experimental setup and measurement methods used in this study are explained in Section 2. The problem is formulated and three hypotheses are introduced based on available theories in Section 3. The experimental results are presented in Section 4 followed by a comparison between the hypotheses and experimental data along with an analysis of the effect of the bed proximity and initial displacement on the AMI.

2. EXPERIMENTAL SETUP AND PROCEDURE

2.1. General setups

Experiments were conducted in a water tank; whose dimensions are 1 meter in length and 30 cm in width. The depth of the test section is 30 cm. However, changing the depth of water makes it possible to control the wet length (L_w) of the cylinder. The cylinder cross section is circular with outer diameter of D=3 cm and mounted vertically as a surface-piercing circular column.

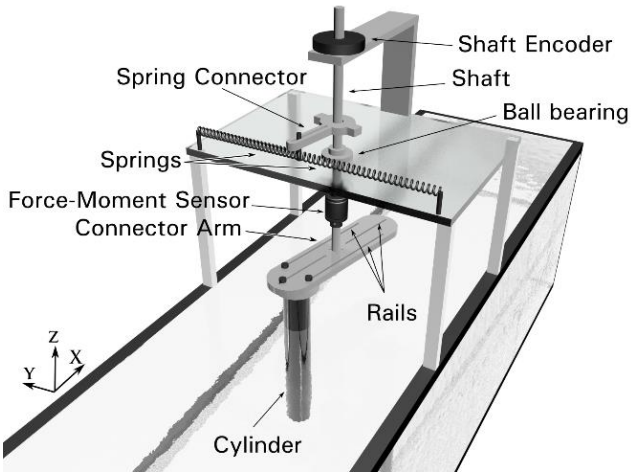

Fig. 1 3D view of experimental setup.

Different parts of the apparatus are shown in **Error! Reference source not found.**. The cylinder is pivoted outside of the water through a connector arm, using a rigid shaft and a ball bearing. It has one degree of freedom with linear rotational variation around the Z axis. The top end of the cylinder is fixed on the connector arm's rails by using three screws, allowing us to slide the cylinder along the arm and adjust the arm length (l) and as a result, the moment of inertia of the system. Two linear springs are connected to the shaft by using a spring connector arm to act as restoring moment. There are two sensors connected to the shaft, measuring angular rotation and force-moments acting on the shaft at the same time.

The first sensor is a shaft encoder, which measures angular rotation by using two optical sensors and an encoder disk. There is no physical contact between the shaft and the encoder, hence there is no damping induced by the encoder.

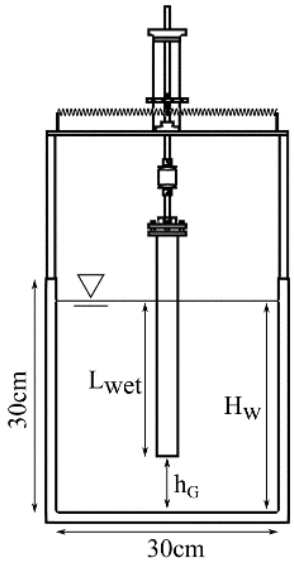

Fig. 2 Front view of the experimental setup.

The second sensor is a 6-DOF force-moment sensor which is able to measure forces and moment acting on the shaft.

To determine principal characteristics of the system, free decay tests were performed outside of water with and without springs connected.

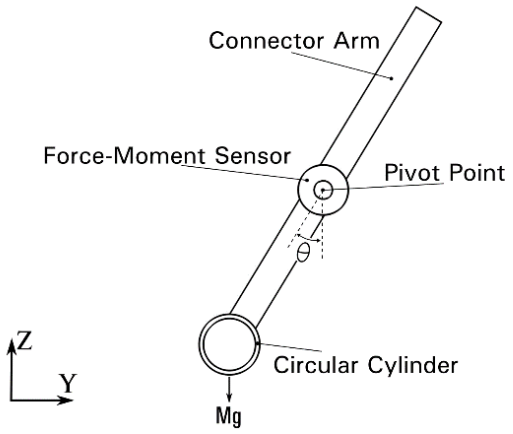

Fig. 3 Side view schematic of the pendulum setup of the apparatus.

To estimate the moment of inertia of the apparatus without the cylinder (I_0), the apparatus is setup vertically without the springs connected as shown in **Error! Reference source not found.** while the cylinder is connected at the maximum arm length. Since the springs are disconnected the system can swing freely like a physical pendulum. By releasing the cylinder after an initial displacement (Θ0), the response is recorded and used for determining the total mass moment of inertia. Then I0 is calculated by using parallel axis theorem:

$$I = I_{cm} + Ml^2 \tag{1}$$

Where I_{cm} is the moment of inertia around the central axis, M is the mass of the rotating body and l is the perpendicular distance between the central axis and the pivot point.

The restoring mechanism of the apparatus consists of two linear springs and a connector arm. Although the springs are linear, the relation between the total restoring moment and displacement is nonlinear due to the configuration of the springs. To find the stiffness of an equivalent torsional spring as a function of displacement, the total stiffness of the restoring mechanism is measured by using the force-moment sensor in different rotation angles. Then the best polynomial fit is calculated based on the recorded data by using MATLAB software and then used to determine the restoring moment as a function of displacement.

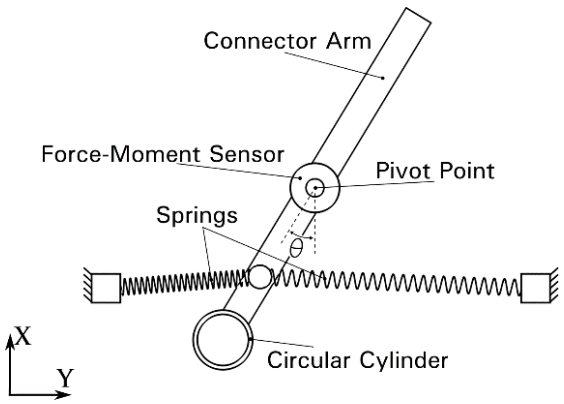

Fig. 4 Plan view schematic of the cylinder with springs connected.

To evaluate the total structural damping C_{str}, free decay tests were carried out outside of water in horizontal setup with springs connected as shown in **Error! Reference source not found.**. To reduce the effect of air drag force, the cylinder is disconnected during the horizontal free decay tests.

2.2. Procedure

In-water tests were carried out by releasing the cylinder after an initial displacement (Θ_0) inside of water. The output voltage of both sensors is recorded via a data logger at the same time and then analyzed in MATLAB software. An ultra-precise position estimation method is implemented to calculate the rotation and angular velocity accurately (Kim et al., 2006). The output signal of the force-moment sensor is also converted to force and moments by using a calibration matrix provided by the manufacturer of the sensor.

A general approach to free decay tests is to maintain small angular displacements during the test assuming that damping effect would not cause significant error in the resulting estimate of the moment of inertia. The procedure is to measure the average oscillation frequency over many oscillations and estimate the moment of inertia from the solution to the linearized equation of motion.

In this paper, parameter estimations were made by using MATLAB nonlinear least square curve fitting function "lsqcurvefit", such that the difference between the simulated model output and experimental data is minimized according to a user-chosen criterion. The workflow for parameter estimation is as follows:

1. Develop a dynamic model of the system under test. The inputs and outputs of the dynamic model must correspond to the inputs and outputs of the experiments to be run on the system.

2. Use MATLAB parameter estimation to import and pre-process the experimental data to prepare for parameter estimation. In the experimental runs for this paper, the first few raw data points were removed so that the experimental data would begin at rest.

3. Choose the parameters and appropriate optimization options (sum of squared errors in this case) and run the parameter estimations.

Solving the nonlinear equation of motion removes some of the restrictions of using simplified equation of motion and produces more accurate results in a least-square error sense.

3. FORMULATION OF THE PROBLEM

The rotating body shown in **Error! Reference source not found.** is simplified by using equivalent torsional spring as shown in Fig. 1. The effects of hydrodynamic forces on a submerged body shown in Fig. 1 include: (a) drag force and the drag induced moment and (b) added mass and the AMI. Similarly, the structural forces acting on the body include: (c) the spring restoring moment and (d) the structural damping. The buoyancy and gravity forces are neglected since they do not produce any torque around the pivot point.

The total drag force is consisted of shear drag, pressure drag, and wake induced force. The shear drag force is the integral of wall shear stress around the body surface as shown in gray in Fig. 1:

$$\tau_w = 2\pi r^2 L_{wet} \mu \frac{du}{dr} \tag{2}$$

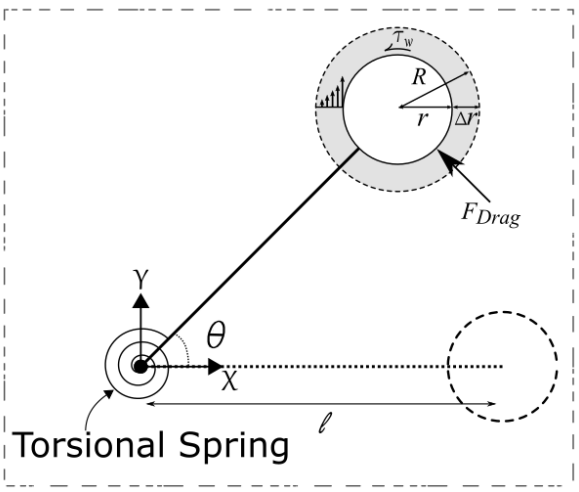

Fig. 1 Schematic diagram of the pivoted cylinder.

Where L_{wet} is the length of cylinder interacting with water, μ is the kinematic viscosity of water and r is the radius of the cylinder. Assuming the fluid velocity drops to zero at a distance Δr from the body and no slip boundary condition on the cylinder wall, the shear moment around the pivot point becomes:

$$\tau_w = \frac{\int_{\dot{\theta}r}^{0} 2\pi L_{wet}\mu du}{\int_r^R r^2 dr} = \frac{2\pi L_{wet}\mu r^2 R\dot{\theta}}{\Delta r} \tag{3}$$

Where dot symbol stands for differentiation with respect to time and l is the distance between the pivot point and central axis of the cylinder. Since the total area of the end cap of cylinder is negligible compared to the total surface area, the shear force on the end face is neglected.

To determine Δr, the shear moment is measured by fixing the cylinder at the center of the connector arm during free decay test to eliminate the effect of the drag force. The quadratic drag moment around the pivot can be expressed as:

$$\tau_d = \rho\pi r L_{wet} C_D (l\dot{\theta})^2 l \tag{4}$$

Where the drag coefficient C_D is estimated in each test by using optimization technique as explained in Section 2 In general, at low Reynolds numbers, the sum of pressure and skin-friction drag on a bluff or blunt body is much greater than wake induced drag force and the wake induced force is negligible compared to the total drag force. In this study, the maximum Reynolds number is around 2000, therefore the effect of wake induced force is not significant.

The extra hydrodynamic forces caused by accelerating the fluid can be calculated based on experiment by using the equation of motion:

$$\sum \tau = (I + I_a)\ddot{\theta} \tag{5}$$

Where I_a is the AMI. Here, we introduce three different hypotheses for estimating the AMI in this study. In the first hypothesis, it is assumed that the AMI of the cylinder, equals to the moment of inertia of a displaced volume of water, concentrated on the center of gravity of the cylinder (I_{Po}). This hypothesis does not consider the distribution of the mass and therefore, the first term in (5) becomes zero and calculated AMI is similar to potential flow results.

In the second hypothesis, a cylinder of water with circular cross section is assumed as displaced volume of water and the moment of inertia of this displaced volume is assumed to be the AMI (I_{Cy}).

In the third hypothesis, a cylindrical tube of water is assumed to move with the cylinder as a more realistic approach. By assuming that the cylindrical tube of water has the same length as the moving cylinder, it's possible to calculate Δr, since it's assumed that the cylindrical tube mass is equal to the displaced mass of water. Then, the moment of inertia of the cylindrical tube volume is assumed to be the AMI (I_{Tu}).

Similar to the added mass coefficient C_a, the AMI coefficient is introduced here as:

$$C_A = \frac{I_a}{I_{Cy}} \tag{6}$$

Since I_{Po} is zero when the cylinder rotates around the central axis, I_{Cy} is used for normalizing the added mass moment of inertia instead of I_{Po}.

The spring moment is a function of the spring stiffness and the position of the moving body. Here the restoring system consists of two linear spring connected to the shaft through a connector arm as shown in **Error! Reference source not found.**. The spring restoring moment is:

$$\tau_{Spring} = K_\theta \theta \tag{7}$$

Where K_Θ is the equivalent torsional spring stiffness.

The structural damping is calculated based on decay tests in air without connecting the cylinder to reduce the effect of air drag on the vibrating system. Since most of the dissipated energy is absorbed by the ball bearings and spring internal friction, the damping is represented as coulomb (frictional) damping:

$$\tau_f = \tau_r C_{str} \mathrm{sgn}(\dot{\theta}) \tag{8}$$

Where τ_r is the frictional torque induced by ball bearings. τ_f is obtained from pendulum free decay tests in air as explained in Section 2.1. For a rotating body shown in Fig. 1, the equation of motion is:

$$\tau_W + \tau_d + \tau_f + \tau_{Spring} = (I + I_a)\ddot{\theta} \tag{9}$$

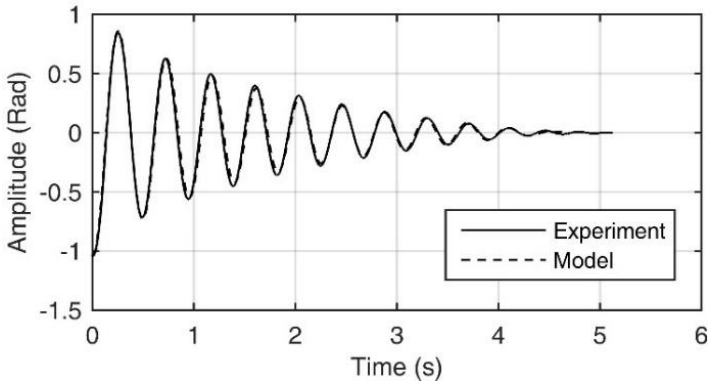

Fig. 2. Experimental results compared with numerical results based on optimization. (l=7.12cm, L_{wet}=13.85cm, h_g=1.15cm and Θ_0=1.04Rad)

From (1)–(9) it's possible to estimate C_D and I_a in each test by using optimization technique if the values of Δr and τ_f are obtained from experiment, as explained in Section 2.2. A comparison between the model and experiment is shown in Fig. 2. One probable reason for the difference between model and experimental result is that the friction torque and damping torque actually depended on the frequency; however, this dependency is not included in our model.

4. RESULTS AND DISCUSSION

To find the best hypothesis to estimate the AMI the introduced hypotheses are compared with the experimental results.

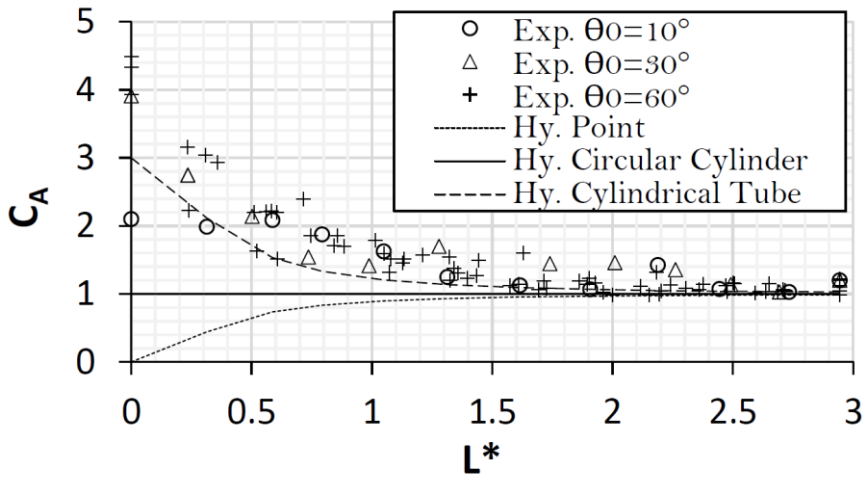

Fig. 3 AMI coefficient (CA) as a function of the arm length ratio

Fig. 3 shows the experimental results for three different initial displacements (Θ_0) and three hypotheses we made in Section 3. Based on Fig. 3, all hypotheses are converging to the experimental results by increasing L^*, because the cylinder resembles a point and the mass distribution is less effective, notably for $L^*>1$.

However, cylindrical tube hypothesis gives the best approximation compared to other hypotheses, specifically when the pivot point is close to the center ($L^*<1$).

4.1. The effect of end gap (hg)

To study the effect of bed proximity, decay tests were done for four different gap ratios (h_g/L_{wet}) while wet length of the cylinder is constant (L_{wet}=0.139 m) and initial displacement is 60° in all tests.

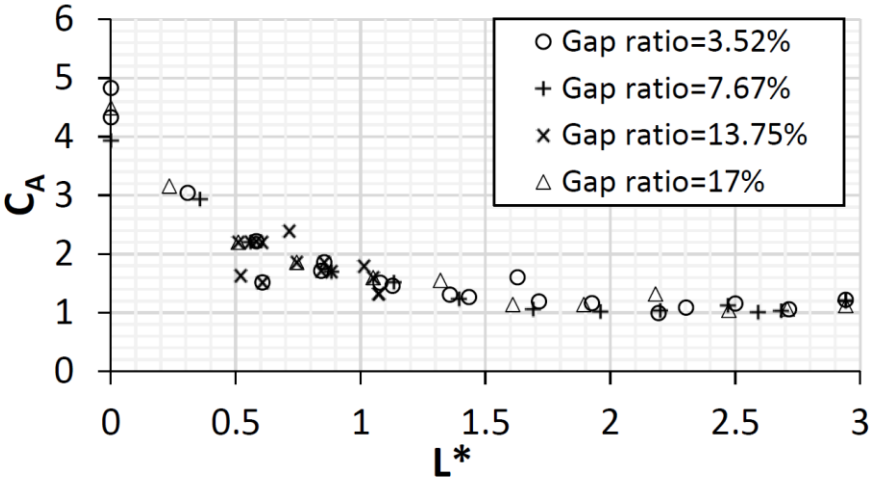

Fig. 4 AMI coefficient (C_A) as a function of arm length ratio (L^*). L_{wet}=0.139 m and initial displacement is 60°.

According to Fig. 4, The AMI coefficients are almost identical regardless of the gap ratio. The bed proximity effect is insignificant because the diameter of the cylinder is relatively small and the area of the end cap is negligible compared to the total surface area of the cylinder.

4.2. The effect of initial displacement

Changing the initial displacement affects the maximum relative velocity between the cylinder and fluid and as a result the drag force. This effect is studied by keeping the gap ratio constant (18.2%) during the test.

The results for three initial displacements are shown in Fig. 5. According to the results, C_A is close to the circular cylinder hypothesis results for Θ_0=10° (C_A=1). However, the results for Θ_0=30° and Θ_0=60° are almost similar and diverge from those for Θ_0=10° almost equally, specifically for $L^*<1$. Although more tests are needed for determining the effect of initial displacement on AMI, circular cylinder hypothesis is reliable for initial displacements less than 10° and $L^*>1$.

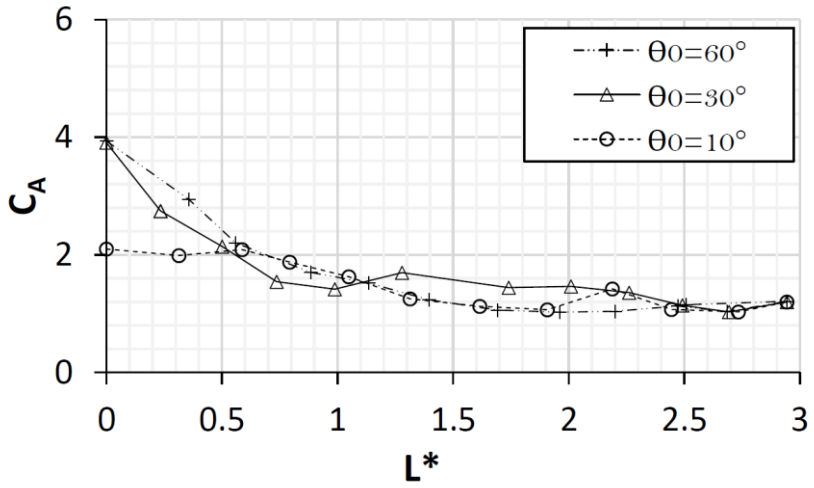

Fig. 5 Experimental results of AMI coefficient (C_A) as a function of arm length ratio (L^*) for different initial displacements. (gap ratio=18.2%)

5. CONCLUSION

For the determination of total added mass moment of inertia (AMI) of a rotating body, a surface piercing vertical cylinder is used which is pivoted at distance l. The problem is mathematically formulated by using three different hypotheses treating the cylinder as 1) point, 2) circular cylinder and 3) cylindrical tube. Then parameter estimations were made by using MATLAB nonlinear least square curve fitting function "lsqcurvefit", such that the difference between the simulated model output and experimental data is minimized.

The results show that all hypotheses are converging to the experimental results by increasing L^*. However, cylindrical tube hypothesis gives the best approximation compared to other hypotheses, specifically when the pivot point is close to the center ($L^*<1$).

It is also confirmed that the AMI coefficients are almost identical regardless of the gap ratio according to decay tests.

It is found that for initial displacement of $\Theta_0=10°$, C_A is close to the circular cylinder hypothesis results ($C_A=1$). However, by increasing initial displacement to $\Theta_0=30°$ and $\Theta_0=60°$ the results are almost similar and diverge from those for $\Theta_0=10°$ almost equally, specifically for $L^*<1$. Although more tests are needed for determining the effect of initial displacement on AMI, in conclusion, circular cylinder hypothesis is more reliable for initial displacements less than 10° and $L^*>1$.

ACKNOWLEDGMENT

This study was financially supported by the Grant-in-Aid for Scientific Research 15H04211.

REFERENCES

[1] S. H. Lamb, Hydrodynamics, 6th Editio. Cambridge University Press, 1959.
[2] K. Wendel, "Hydrodynamic Masses and Hydrodynamic Moments of Inertia," Jahrb. d. STG, vol. 44, 1950.
[3] Proudman, "Rotating Log of Square Section in an Infinite Fluid," Trans. Inst. Nav., p. 80, 1916.
[4] Weinblum, "Die Bewegungsgleichungen des Schiffes im Seegang," Schiffbau, p. 529, 1931.
[5] J. Melorose, R. Perroy, and S. Careas, Flow-Induced Vibrations: Classifications and Lessons from Practical Experiences Second Edition, vol. 2. 2015.
[6] F. Flemming and C. H. K. Williamson, "Vortex-induced vibrations of a pivoted cylinder," J. Fluid Mech., vol. 522, pp. 215–252, Jan. 2005.

[7] H. G. Sung, H. Baek, S. Hong, and J.-S. Choi, “Numerical study of vortex-induced vibration of pivoted cylinders,” Ocean Eng., vol. 93, no. 2015, pp. 98–106, 2015.

[8] J. S. Wu and M. Hsieh, “An experimental method for determining the frequency-dependent added mass and added mass moment of inertia for a floating body in heave and pitch motions,” Ocean Eng., vol. 28, no. 4, pp. 417–438, 2001.

[9] J. C. Kim, J. M. Kim, C. U. Kim, and C. Choi, “Ultra Precise Position Estimation of Servomotor using Analog Quadrature Encoders,” Twenty-First Annu. IEEE Appl. Power Electron. Conf. Expo. 2006. APEC ’06., no. 4, pp. 930–934, 2006.